

PAPER

Improving energy harvesting by nonlinear dual-beam energy harvester with an annular potential energy function

To cite this article: Nan Shao *et al* 2023 *Smart Mater. Struct.* **32** 015018

View the [article online](#) for updates and enhancements.

You may also like

- [Cellular automaton traffic model considering driver's reaction to velocity and headway distance with variable possibility of randomization](#)
Guoqiang Zhang and Weiling Xu
- [A four-channel microelectronic system for neural signal regeneration](#)
Xie Shushan, Wang Zhigong, Lü Xiaoying et al.
- [Implementation of energy conservation in a commercial building using BEM and sub-metering technology](#)
Chao Wang, Zhenqian Chen, Zhichao Tian et al.

ECS Toyota Young Investigator Fellowship



For young professionals and scholars pursuing research in batteries, fuel cells and hydrogen, and future sustainable technologies.

At least one \$50,000 fellowship is available annually.
More than \$1.4 million awarded since 2015!



Application deadline: January 31, 2023

Learn more. Apply today!

Improving energy harvesting by nonlinear dual-beam energy harvester with an annular potential energy function

Nan Shao¹ , Hongxin Yang¹, Zhen Huang¹, Jiawen Xu^{1,*} , Xiaosu Xu¹ and Ruqiang Yan²

¹ School of Instrument Science and Engineering, Southeast University, Nanjing, Jiangsu 210096, People's Republic of China

² International Machinery Center, School of Mechanical Engineering, Xi'an Jiaotong University, Xi'an, Shaanxi 710049, People's Republic of China

E-mail: jiawen.xu@seu.edu.cn

Received 10 September 2022, revised 23 October 2022

Accepted for publication 6 December 2022

Published 20 December 2022



CrossMark

Abstract

In this paper, we develop a nonlinear dual-beam energy harvester for broadband energy harvesting. Two identical piezoelectric cantilevers are placed orthogonal to each other and coupled by repulsive magnetic force. Analytical and experimental studies indicate that the combination of the resonant motions of the two beams yields an annular potential energy function, where the oscillator can circumambulate around the potential barrier. The advantages of the design concerning a conventional bistable piezoelectric cantilever were examined. It is proved that the proposed harvester has a bandwidth of 3.4 Hz and a voltage output performance 298.7% better than that of a bistable one under excitations of 0.5 g.

Supplementary material for this article is available [online](#)

Keywords: piezoelectric energy harvesting, magnetically coupling, nonlinear vibration, annular-stable, inter-well modulation

(Some figures may appear in colour only in the online journal)

1. Introduction

Vibration energy harvesting is a potential solution for powering the Internet of Things sensors [1]. A typical vibrational energy harvester is a second-order resonator with optimal performance at a single frequency point [2, 3]. Researchers proposed various approaches to broadening the operating bandwidth of the harvesters [4], including resonant frequency tuning [3–6], introducing Duffing-type nonlinearity [7–10], frequency-up conversion [11, 12], multimodal [13], and internal resonance [14–16], etc. Duffing-type

piezoelectric energy harvesting (PEH) received the most significant attention [17]. Stanton analyzed the softening and hardening responses of a monostable PEH for broadband energy harvesting [18]. It was revealed that a typical bistable PEH has a wider bandwidth than a monostable one due to inter-well oscillations. In particular, the bistable PEHs have promising advantages for harvesting low-frequency vibration energy [19–21]. In addition, Litak analyzed the characteristics of a bistable PEH under random excitation [22]. Masana demonstrated the potential shape-dependent performance of a harvester in mono- and bi-stable states [23].

On the other hand, conventional bistable PEHs need to gather a large amount of mechanical energy for the inter-well jumping motion, i.e. they have optimal performances under

* Author to whom any correspondence should be addressed.

large amplitude excitations only [8, 23]. To address this issue, investigations were carried out focusing on modifying the shape of the potential barriers. For instance, Leademham and Erturk developed an M-shaped energy harvester by reducing the barrier of the potential well [24]. Besides, a potential well with multiple stable states would enable large amplitude motion [25]. Moreover, it was demonstrated that external impact forces can trigger a jumping motion [26]. More recently, Zhou *et al* proposed a bi-stable energy harvester with a variable potential well that has a smaller threshold for snap-through [27]. Inter-well modulation is used to reduce the barrier height and make inter-well oscillation easier to achieve [28–31]. Nevertheless, the bistable PEHs must climb over the potential barrier.

Ideally, a PEH does not need to jump over a potential barrier when passing the central point while the features of bi-stability are maintained for large amplitude motion. In this research, we introduce a secondary beam with identical parameters that are placed orthogonal to the primary one and couple their resonant motions by repulsive magnetic force. We hypothesize that the magnetic force will make the secondary beam resonant to the furthest point when the primary beam approaches the center position, thereby minimizing the barrier of potential energy. Meanwhile, the secondary beam would resume to the central point that yields significant bi-stability for generating large amplitude motion. In other words, the system can circumambulate around the potential barrier rather than jump over it. In such a case, the PEH does not need to gather a large amount of energy. Hence the voltage output performance of both the beams is expected to be enhanced over a wide frequency range under small vibration.

The rest of the paper is organized as follows. The structural design and working principle are outlined in section 2. Theoretically, modeling is presented in section 3 and the two-dimensional potential function is analyzed theoretically in section 4. Simulations, experimental studies, and discussions with a comparison of a bistable one are presented in section 5. Concluding remarks are given in the last section.

2. Structural design and working principle

The schematic and experimental set-up of the proposed two-dimensional PEH is presented in figures 1(b) and (c). The PEH consists of two identified piezoelectric cantilever beams placed orthogonal to each other. Permanent magnets and two pieces of lead zirconate titanate (PZT) sheets are attached to the tip and root of the beams, respectively. Here beam A vibrations in the x -direction and beam B vibrations in the y -direction. Besides, the repulsive force between the two magnets is chosen for generating a two-dimensional interaction between the beams.

In this study, we utilize the coupling of the motions in orthogonal directions to create an annular two-dimensional potential well. From the view point of a single beam, one beam encounters a minimized potential barrier when it approaches

the center position as the other beam moves to the furthest point. At the system level, the combined motion of the two beams circumambulates around the potential barrier in the two-dimensional space. For comparison, a conventional bistable PEH with beam B fixed was modeled and experimentally studied, as shown in figures 1(a) and (d).

3. Modeling and experimental setup

We focus on the first bending vibration mode for beams' motion. The beam model is built using the Euler–Bernoulli beam theory. The displacements of beam A and beam B are $w_1 = \phi_1(z_1)q_1(t)$ and $w_2 = \phi_2(z_2)q_2(t)$, where $\phi_i(z_i)$ and $q_i(t)$ are the mode shape function and modal displacement of the i th beam. Besides, $x = w_1(L, t)$ and $y = w_2(L, t)$ stands for the displacement of the tips of the two beams. The governing equations of the system are given

$$m_1\ddot{x} + c_1\dot{x} + k_1x + \frac{\partial U_m(x, y)}{\partial x} + \chi_1 V_1 = -m_1 a_x \quad (1)$$

$$\frac{V_1}{R_1} + C_1^S \dot{V}_1 - \chi_1 \dot{x} = 0 \quad (2)$$

$$m_2\ddot{y} + c_2\dot{y} + k_2y + \frac{\partial U_m(x, y)}{\partial y} + \chi_2 V_2 = -m_2 a_y \quad (3)$$

$$\frac{V_2}{R_2} + C_2^S \dot{V}_2 - \chi_2 \dot{y} = 0 \quad (4)$$

where V_i is the voltage output, m_i is the equivalent mass, c_i is the equivalent damping, k_i is the equivalent stiffness, χ_i is the electromechanical coupling term, C_i^S is the capacitance of the piezoelectric plate, and R_i is the load resistance of the i th beam, respectively. The lumped parameters of the proposed PEH system can be calculated by adopting the usual assumed-mode approach [2]. Besides, a_x and a_y are the excitations in the x - and y -direction, respectively. It is worth noticing that, the freedoms of motion in two-dimensional space would yield a two-dimensional magnetic field. The magnetic field can be described by the dipole–dipole model [32]

$$U_m(x, y) = \frac{\tau M_1 M_2}{2\pi} (x^2 + y^2 + D^2)^{-\frac{3}{2}} \quad (5)$$

where M_1 and M_2 are the moments of the magnetic dipoles of the magnets attached to the two beams, respectively, τ is the vacuum permeability, and D is the distance between the magnetic dipoles. As repulsive force is adopted, we have moments of the magnetic dipoles $M_1 = M_2$. In this article, $M_1 = M_2 = 0.346 \text{ A} \cdot \text{m}^2$, $\tau = 4\pi \times 10^{-7} \text{ H m}^{-1}$ are chosen. The geometric parameter of the magnet is 1 cm in diameter and 1.2 cm in thickness, and the physical parameter is the magnetic field strength of 4589 Gs. Thus, the total potential energy of the mechanical system is given

$$U(x, y) = U_m(x, y) + \frac{1}{2}k_1x^2 + \frac{1}{2}k_2y^2. \quad (6)$$

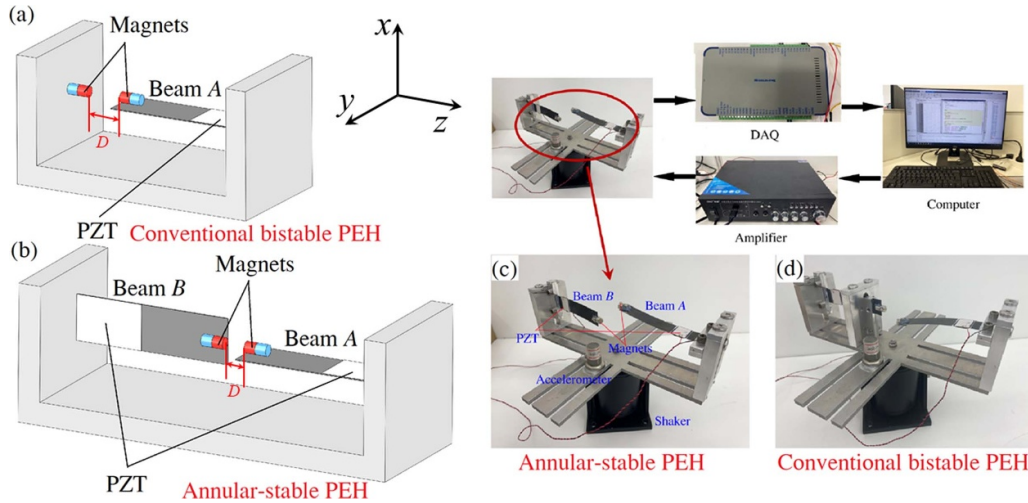


Figure 1. Schematics and experimental set-up of (a) a conventional bistable PEH; (b) the annular-stable PEH with potential well in two-dimensional space; experimental set-up of (c) the annular-stable PEH and (d) a conventional bistable PEH.

Table 1. Parameters of the experimental set-up.

Cantilever beam size (mm ³)	95 × 20 × 0.2
Piezoelectric transducer size (mm ³)	15 × 20 × 0.3
Electromechanical coupling ($\mu\text{N V}^{-1}$)	163.69
Capacitance (nF)	11.0

It can be obtained from equations (5) and (6) that the potential function is a central symmetry one when k_1 equals k_2 . Note the stiffness of the two beams are constant values for a given mechanical configuration. We can adjust the potential well by modifying the magnetic field. Besides, the magnetic coupling provides additional stiffness to the two beams. And the stiffness of one beam is depending on the displacement of the other one.

Analytical and experimental studies are then carried out on the prototype of the annular-stable PEH to elucidate the response characteristics. Without loss of generality, responses of the system under x -direction excitation are focused on in the following discussion due to the symmetry of the PEH. The parameters of the system are listed in table 1. Stainless steel sheets were chosen as the substrate for the two beams. Two PZT-5 A sheets were respectively glued at the roots of beam A and beam B using epoxy glue (DP420). In the experiment, the system was mounted onto a shaker which was driven by a power amplifier. The distance between the two magnets in the z -direction was adjusted to 15 mm. A constant excitation with an amplitude of $a = 0.5 \text{ g}$ was chosen ($g = 9.8 \text{ m s}^{-2}$). The amplitude of based movement was measured and controlled by an accelerometer (CT1020LC, ChengTec). It is worth emphasizing that 0.5 g is small one. A typical bi-stable PEH may require excitation with amplitude over 10 m s^{-2} for triggering the inter-well motion [23, 26]. Besides, probes with input impedance of $R = 10 \text{ M}\Omega$ were adopted in the experiments, i.e. the harvesters were tested in an open circuit condition. The resulting voltage outputs of the system were measured with a sampling frequency of 10 kHz. Moreover, the

amplitudes of the output voltages of the piezoelectric transducers attached to beam A and beam B were measured and recorded under excitations with steps of 0.2 Hz. In addition, analytical frequency responses were simulated using the Runge–Kutta method in MATLAB.

4. Analysis of potential function

The key advantage of the proposed system stems from the potential well in two-dimensional space. We firstly analyzed the potential well analytically. Notably, the two-dimensional system may have monostable and annular stable states depending on the distance between the two magnets. In particular, the system has an annular-stable state, distinct from the bistable one, with a properly selected distance between the two magnets, as shown in figure 2.

Figure 2 depicts the theoretical potential energy of the proposed PEH in the two-dimensional space. It can be obtained that the system has a circular-shaped potential well when the distance D is 15 mm. Besides, a conventional bistable PEH has a one-dimensional potential well with two stable points and a potential barrier between them, as shown in figure 2(c). The conventional harvester must jump over the barrier for the inter-well motion. In this study, the proposed PEH has a circular-shaped stable line and a potential barrier at the center of the two-dimensional energy. The two-dimensional potential well would enable a motion that the oscillator would circumambulate around the potential barrier rather than jump over it. Consequently, the oscillator does not need to gather a large amount of mechanical energy for the jumping motion, enabling large amplitude vibration under small excitations. Besides, the locations of the circular-shaped stable line are dependent on the distance between the two magnets, as shown in figure 2(d). In particular, the system is a monostable one when D is larger than 17.8 mm. And it switches into the annular stable one with a smaller D . And the radius of equilibria increases with the decrease of D . It is worth mentioning that many other factors

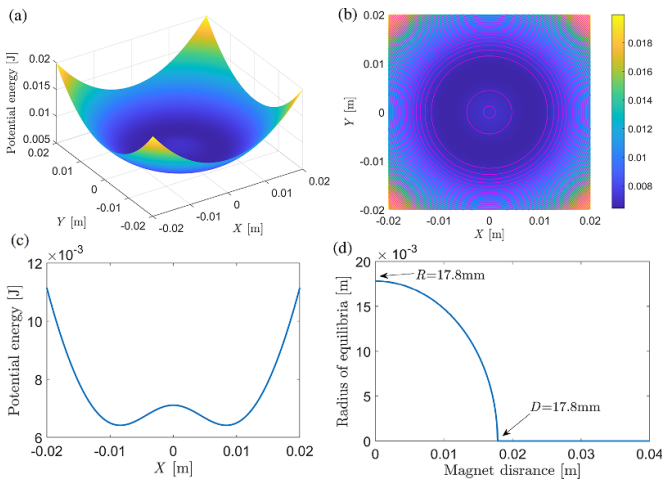


Figure 2. (a) The two-dimensional potential energy of the proposed PEH, (b) the top view of the two-dimensional potential energy, (c) the one-dimensional potential energy of a bistable PEH, and (d) the radius of the equilibria vs the magnet distance D .

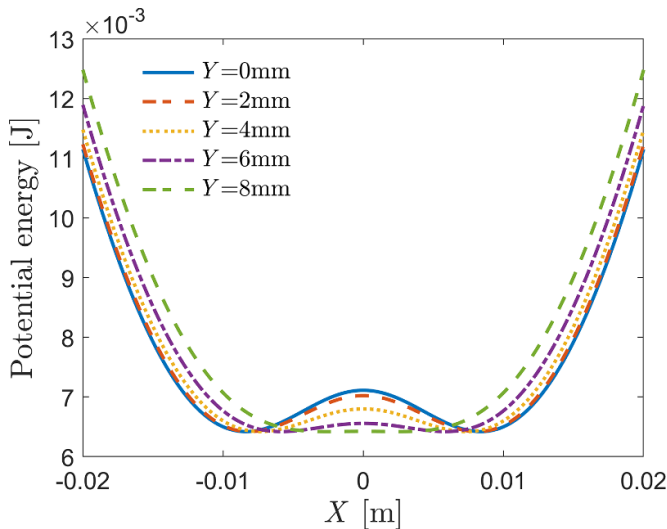


Figure 3. Shapes of the potential well of beam A with $D = 15$ mm and different Y .

would influence the potential energy function. For example, increasing the stiffness of beams A and B can reduce the height of the potential barrier. Besides, a difference in the stiffnesses of beams A and B would lead to mismatching between the two beams and therefore reduce the coupling efficiency.

From the viewpoint of a single beam, the potential curve for each beam is a dynamic one depending on the displacement of the other beam, as shown in figure 3. The real-time potential well for a single beam would be a one-dimensional cross-section curve of the two-dimensional potential wells. We take an example of the system in an annular stable state when $D = 15$ mm. It can be obtained that changing the displacement of beam B results in different shapes of the potential well for beam A. It can be obtained that the potential well has a large peak when the displacement Y is 0 mm and 2 mm.

Meanwhile, the shape of the potential well becomes a flat one when $Y = 6$ mm. Notably, the two beams have significant energy interchange during their resonant motions. And the displacement of beams A and B would have a phase difference approximating $\pi/2$, as would be demonstrated in section 5. Therefore, beam A would encounter no potential barrier when passing through the central point. It has a significant advantage over the bistable PEH with a flexible potential function where a potential barrier remains throughout the operation of the PEH [27]. Besides, the benefits of bi-stability can be maintained when the beam has a large displacement. In contrast, the bistable PEH has a constant potential well and it would be difficult to jump over the barrier.

5. Numerical and experimental analysis

The two-dimensional potential well yields a system-level circular-shaped motion. Here we compare the responses of the annular-stable PEH with a conventional bistable one. Voltage outputs are simulated and measured. The responses are obtained at 11.2 Hz under excitation of 0.5 g, i.e. at the frequency point with large outputs for the two systems. Figure 4 presents the time-domain responses, the responses in two-dimensional space of the displacements and voltage outputs of beam A and beam B and the corresponding phase portraits. It can be obtained that the proposed PEH has circular-shaped motion in two-dimensional space for both the displacement and voltage output responses. It demonstrates that the proposed system has large amplitude oscillation in the annular-stable state at the selected frequency point. Besides, beams A and B have similar voltage outputs in the steady state response. And the phase difference between the voltage output of beam A and beam B is close to $\pi/2$, as shown in figures 4(g)–(i). This phenomenon indicates that the proposed system has a much smaller variation of system-level potential energy than that of the conventional bistable one. In other words, the proposed PEH does not need to gather a large amount of mechanical energy for the large amplitude motion. In addition, it can be obtained from the responses in two-dimensional space that the dynamics of the annular-stable PEH combine radial- and tangential-direction motions along the circular-shaped potential well. The measured results match with the simulated one well. A minor difference exists in the phase difference of beams A and B between the measured results and the simulated one, as shown in figures 4(g) and (h).

For comparison, figures 4(d)–(f) present the measured and simulated time-domain responses of a conventional bistable PEH. It can be obtained that the conventional bistable PEH has a much smaller voltage output than that of the proposed PEH under 0.5 g. This is because the bistable PEH has intra-well motion only due to the small amplitude excitation. Figure 4(j) presents the phase portraits of the proposed PEH and the conventional bistable PEH. It is shown that beams A and B can vibrate over a wider range than that of the bistable one. Notably, the two-dimensional motion of the proposed PEH is indeed circular. In other words, the proposed PEH is capable

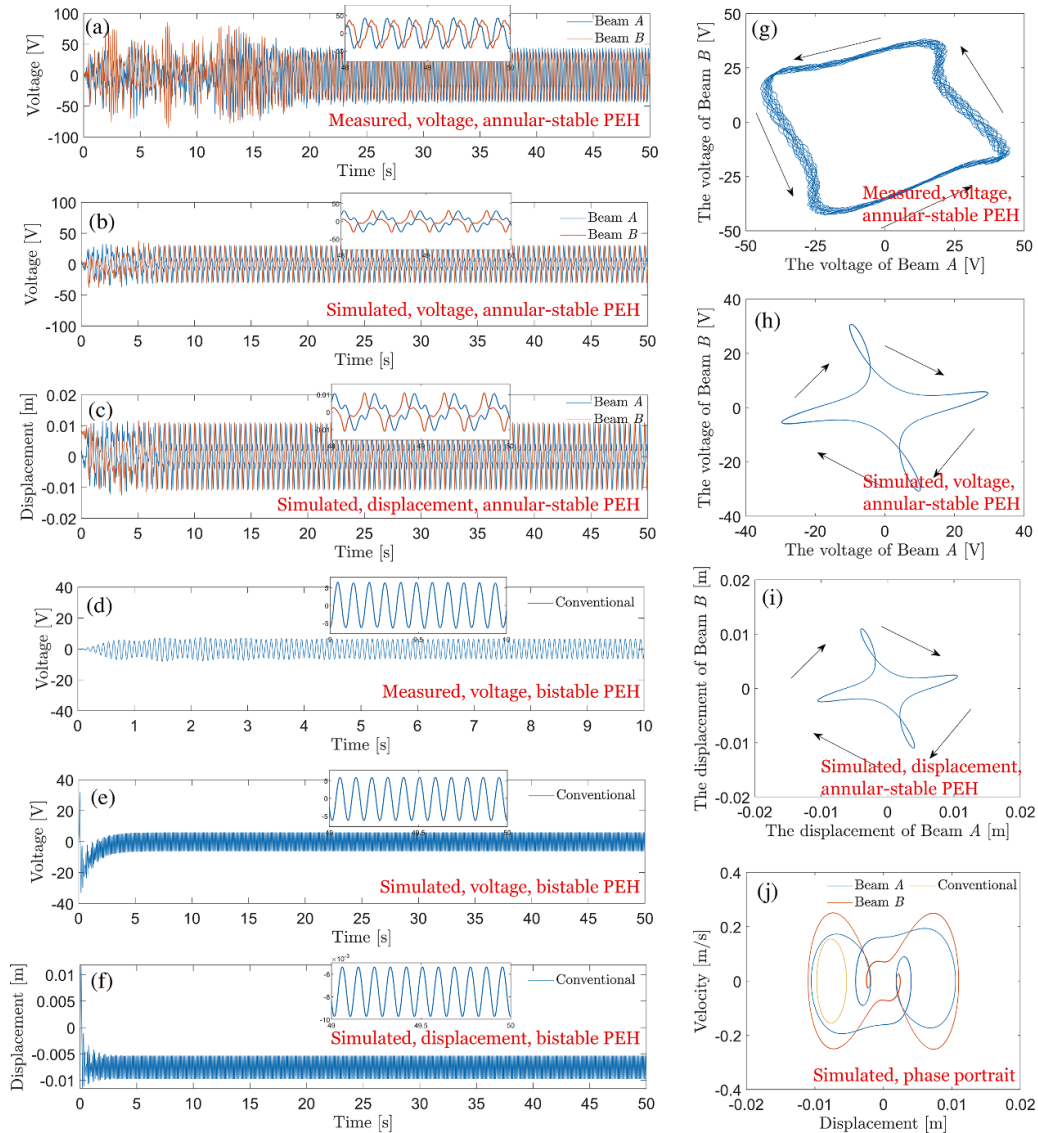


Figure 4. Time-domain response of (a) experimental voltage output and (b) simulated voltage output, and (c) simulated displacement of the annular-stable PEH; (d) experimental voltage output, (e) simulated voltage output, and (f) simulated displacement of a conventional bistable PEH; (g) experimental and (h) simulated voltage output and (i) simulated displacement in two-dimensional space of the annular-stable PEH, (j) comparison of the simulated phase portrait of the annular-stable PEH and conventional bistable one. All the experiments and simulations are performed at 11.2 Hz under 0.5 g.

of detours around the potential barrier for the large amplitude motion. Moreover, a video of the proposed PEH in the annular-stable state is attached in the supplementary material.

The advantages of the annular stable state yield enhanced performance over a wide spectrum, as shown in figure 5. Figure 5 shows the frequency responses of the voltage output (peak–peak value) of a linear system, the conventional bistable PEH, and the proposed annular-stable PEH. Here the linear system denotes a standalone beam A without magnetic coupling. The experimental results are presented in figure 5(a). The simulation results are shown in figure 5(b) for verification. It can be obtained that both beams A and B of the proposed PEH have large amplitude voltage outputs over a wide spectrum. In particular, beam A has a peak voltage output of 95.6 V

with a bandwidth of 3.4 Hz. Moreover, there is a strong coupling between beam A and beam B. Hence beam B has a peak voltage output of 92.4 V. As for comparison, the conventional bistable PEH has a maximum voltage output of 32 V and a bandwidth of 1.6 Hz experimentally. Meanwhile, a linear PEH has a peak voltage output of 48 V experimentally. That is, the proposed PEH has a performance of 298.7% better than that of the conventional bistable PEH and 199.2% better than that of a linear one. The analytical predictions match that of the experimental studies well.

It is worth noticing that the proposed annular-stable PEH has a rectangular-shaped voltage output. In other words, the proposed PEH is capable to maintain large amplitude voltage output throughout the frequency range of interest. This is

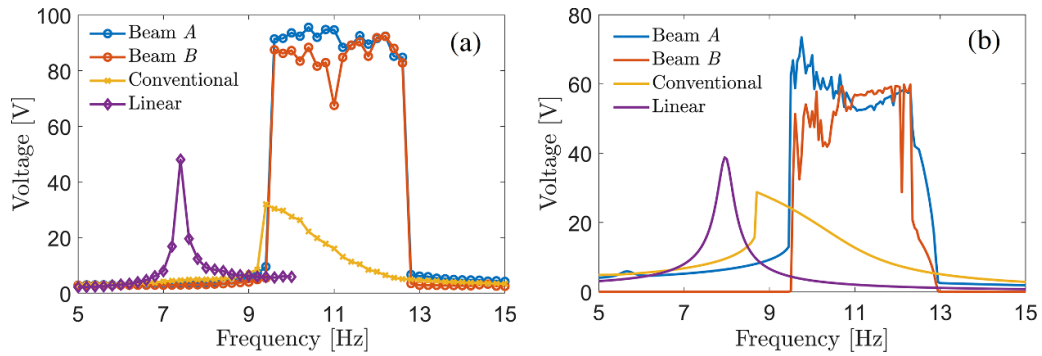


Figure 5. Voltage outputs of a linear system, a conventional bistable PEH, and the annular-stable PEH under $A_x = 0.5g$ and $A_y = 0$: (a) experiment; (b) simulation.

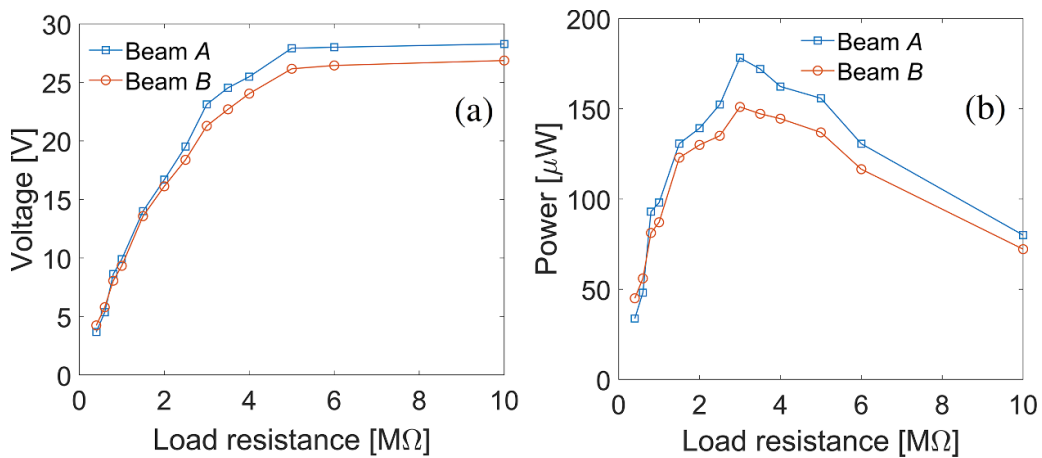


Figure 6. (a) Voltage outputs, and (b) power outputs under different resistance loads under 0.5 g at 11.2 Hz.

because the annular-stable PEH has a large amplitude circular-shaped motion due to the two-dimensional potential well. Meanwhile, the conventional bistable PEH has a triangle-shaped voltage output, i.e. with a peak voltage output at a single frequency point only. It can also be obtained that the proposed PEH and the bistable one has a higher operational frequency range than the linear one. This is because the magnetic field coupling has introduced additional stiffness. It is worth noting that the system's stiffness can be reduced by increasing the length or reducing the thickness of the beam for ultra-low frequency operation.

Figure 6 illustrates root-mean-square voltage outputs versus different resistance loads in the circuit and the power outputs. It was obtained under a stable vibration acceleration of 0.5 g at 11.2 Hz. The maximum energy output values for beams A and B obtained are approximately 178 μW and 151 μW , respectively, with an optimal resistance load of 3 $M\Omega$. The power output of beam A is slightly larger than that of beam B as the excitation comes in the primary vibrating direction of beam A. It is worth mentioning that different resistance loads would lead to the change of the equivalent damping which is potential to impact the bandwidth. On the other hand, the annular-stable PEH is proposed for conceptual illustration and has small system-level electro-mechanical coupling. Hence

the resistance loads have minor influences on the system dynamics. The proposed PEH would be optimized for large electro-mechanical coupling in future research.

6. Conclusion

In summary, a two-dimensional piezoelectric energy harvester, which is comprised of two simple piezoelectric cantilevers, is modeled and analyzed. The two cantilevers are placed orthogonal to each other and be coupled by repulsive magnetic force yielding a two-dimensional potential well. It is shown analytically and experimentally that, with proper selection of the distance between the two cantilevers, an annular stable can be configured with the capability of broadband energy harvesting under small excitations. This feature enables the system to maintain large-amplitude voltage outputs throughout a wide spectrum under small amplitude excitations. It is illustrated that the proposed annular-stable PEH, with a bandwidth of 3.4 Hz, has a performance 298.7% better than that of a conventional bistable one under excitations of 0.5 g. The proposed annular-stable PEH can be extended into applications of multiple directional and wind energy harvesting.

Data availability statement

The data that support the findings of this study are available upon reasonable request from the authors.

Acknowledgments

This work is supported by the National Natural Science Foundation of China Nos. 51905094 and 52275093, the Natural Science Foundation of Jiangsu Province No. BK20190376, and the ‘Zhishan’ Scholars Programs of Southeast University.

Conflict of interest

The authors have no conflicts to disclose.

ORCID iDs

Nan Shao  <https://orcid.org/0000-0003-0181-2409>

Jiawen Xu  <https://orcid.org/0000-0002-5398-0394>

References

- [1] Kim H S, Kim J H and Kim J 2011 A review of piezoelectric energy harvesting based on vibration *Int. J. Precis. Eng. Manuf.* **12** 1129–41
- [2] Erturk A and Inman D J 2009 An experimentally validated bimorph cantilever model for piezoelectric energy harvesting from base excitations *Smart Mater. Struct.* **18** 025009
- [3] Challa V R, Prasad M G, Shi Y and Fisher F T 2008 A vibration energy harvesting device with bidirectional resonance frequency tunability *Smart Mater. Struct.* **17** 015035
- [4] Tang L, Yang Y and Soh C K 2010 Toward broadband vibration-based energy harvesting *J. Intell. Mater. Syst. Struct.* **21** 1867–97
- [5] Al-Ashtari W, Hunstig M, Hemsell T and Sextro W 2012 Frequency tuning of piezoelectric energy harvesters by magnetic force *Smart Mater. Struct.* **21** 035019
- [6] Kim H, Tai W C, Parker J and Zuo L 2019 Self-tuning stochastic resonance energy harvesting for rotating systems under modulated noise and its application to smart tires *Mech. Syst. Signal Process.* **122** 769–85
- [7] Liu H, Lee C K, Kobayashi T, Tay C J and Quan C G 2012 Investigation of a MEMS piezoelectric energy harvester system with a frequency-widened-bandwidth mechanism introduced by mechanical stoppers *Smart Mater. Struct.* **21** 035005
- [8] Tang L and Yang Y 2012 A nonlinear piezoelectric energy harvester with magnetic oscillator *Appl. Phys. Lett.* **101** 094102
- [9] Lan C and Qin W 2017 Enhancing ability of harvesting energy from random vibration by decreasing the potential barrier of bistable harvester *Mech. Syst. Signal Process.* **85** 71–81
- [10] Huang X and Yang B 2021 Improving energy harvesting from impulsive excitations by a nonlinear tunable bistable energy harvester *Mech. Syst. Signal Process.* **158** 107797
- [11] Kulah H and Najafi K 2008 Energy scavenging from low-frequency vibrations by using frequency up-conversion for wireless sensor applications *IEEE Sens. J.* **8** 261–8
- [12] Fu H and Yeatman E M 2019 Rotational energy harvesting using bi-stability and frequency up-conversion for low-power sensing applications: theoretical modelling and experimental validation *Mech. Syst. Signal Process.* **125** 229–44
- [13] Shahruz S M 2006 Design of mechanical band-pass filters for energy scavenging *J. Sound Vib.* **292** 987–98
- [14] Xu J and Tang J 2017 Modeling and analysis of piezoelectric cantilever-pendulum system for multi-directional energy harvesting *J. Intell. Mater. Syst. Struct.* **28** 323–38
- [15] Fan Y, Ghayesh M H and Lu T F 2022 High-efficient internal resonance energy harvesting: modelling and experimental study *Mech. Syst. Signal Process.* **180** 109402
- [16] Xu C and Zhao L 2022 Investigation on the characteristics of a novel internal resonance galloping oscillator for concurrent aeroelastic and base vibratory energy harvesting *Mech. Syst. Signal Process.* **173** 109022
- [17] Sebald G, Kuwano H and Guyomar D 2011 Simulation of a Duffing oscillator for broadband piezoelectric energy harvesting *Smart Mater. Struct.* **20** 075022
- [18] Stanton S C, McGehee C C and Mann B P 2010 Nonlinear dynamics for broadband energy harvesting: investigation of a bistable piezoelectric inertial generator *Physica D* **239** 640–53
- [19] Cottone F, Vocca H and Gammaitoni L 2009 Nonlinear energy harvesting *Phys. Rev. Lett.* **102** 080601
- [20] Erturk A, Hoffmann J and Inman D J 2009 A piezomagnetoelastic structure for broadband vibration energy harvesting *Appl. Phys. Lett.* **94** 254102
- [21] Erturk A and Inman D J 2011 Broadband piezoelectric power generation on high-energy orbits of the bistable Duffing oscillator with electromechanical coupling *J. Sound Vib.* **330** 2339–53
- [22] Litak G, Friswell M I and Adhikari S 2010 Magnetopiezoelectric energy harvesting driven by random excitations *Appl. Phys. Lett.* **96** 214103
- [23] Masana R and Daqaq M F 2011 Relative performance of a vibratory energy harvester in mono- and bi-stable potential *J. Sound Vib.* **330** 6036–52
- [24] Leadenham S and Erturk A 2015 Nonlinear M-shaped broadband piezoelectric energy harvester for very low base accelerations: primary and secondary resonances *Smart Mater. Struct.* **24** 055021
- [25] Kim P and Seok J 2015 Dynamic and energetic characteristics of a tri-stable magnetopiezoelectric energy harvester *Mech. Mach. Theory* **94** 41–63
- [26] Zhou S, Cao J, Inman D, Liu S, Wang W and Lin J 2015 Impact-induced high-energy orbits of nonlinear energy harvesters *Appl. Phys. Lett.* **106** 093901
- [27] Zhou Z, Qin W, Du W, Zhu P and Liu Q 2019 Improving energy harvesting from random excitation by nonlinear flexible bi-stable energy harvester with a variable potential energy function *Mech. Syst. Signal Process.* **115** 162–72
- [28] Lin W, Xu Y, Wang S, Chen Z, Xie Z and Huang W 2022 A nonlinear magnetic and torsional spring coupling piezoelectric energy harvester with internal resonance *Smart Mater. Struct.* **31** 115007
- [29] Yang W and Towfighian S 2017 A hybrid nonlinear vibration energy harvester *Mech. Syst. Signal Process.* **90** 317–33
- [30] Wang Z, Li T, Du Y, Yan Z and Tan T 2021 Nonlinear broadband piezoelectric vibration energy harvesting enhanced by inter-well modulation *Energy Convers. Manage.* **246** 114661
- [31] Yang W and Towfighian S 2018 Low frequency energy harvesting with a variable potential function under random vibration *Smart Mater. Struct.* **27** 114004
- [32] Yung K W, Landecker P B and Villani D D 1998 An analytic solution for the force between two magnetic dipoles *Magn. Electr. Sep.* **9** 39–52